

Oscillatory pairing amplitude and magnetic compressible-incompressible transitions in imbalanced fermionic superfluids in optical lattices of elongated tubes

Kuei Sun and C. J. Bolech

Department of Physics, University of Cincinnati, Cincinnati, OH 45221-0011, USA

(Dated: December 7, 2011)

We study two-species fermion gases with attractive interaction in two-dimensional optical lattices producing an array of elongated tube confinements. Focusing on the interplay of Cooper pairing, spin imbalance (or magnetization) and intertube tunneling, we find the pairing gap can exhibit oscillatory behavior both along the tubes axis and across the tubes, reminiscent of a Fulde-Ferrell-Larkin-Ovchinnikov (FFLO) phase. We obtain a Bose-Hubbard-like phase diagram that shows the magnetization of the system undergoes an incompressible-compressible transition as a function of magnetic field and intertube tunneling strength. We find the parity of tube-filling imbalance in incompressible states is protected by that of the oscillatory pairing gap. Finally, we discuss signatures of this transition and thus (indirectly) of the FFLO pairing in cold atom experiments.

Experimentally trapping and cooling atoms have led to possibilities for studies of condensed quantum many-body systems [1]. Tunable interactions via a Feshbach resonance [2] have provided realizations of paired superfluid states in ultra-cold fermionic gases [3]. Systems of attractive majority and minority spin species (\uparrow and \downarrow , respectively) exhibit various phases distinguishable by the Cooper pairing gap, total density and spin imbalance [4, 5].

One particularly interesting superfluid phase is the Fulde-Ferrell-Larkin-Ovchinnikov (FFLO) state [6, 7] in which the up spins partially pair with the down spins, with a spatially oscillatory pairing amplitude. However, in three dimensions (3D) the FFLO state has remained elusive, while in lower dimensions it can hardly be sustained due to the lack of superfluid long-range order. Recent attention has turned to an array of 1D systems [8–13], which is expected to have both a wider parameter range for the FFLO (as compared with the 3D case) and stabilized long-range order through the coupling between these systems. In cold atom experiments, such arrays have been realized as 2D optical lattices of elongated tube confinements in a global trap [14, 15] (as illustrated in Fig. 1a), with a rich phase diagram observed [15].

On the other hand, bosons in optical lattices have been extensively studied both theoretically and experimentally [1]. A well-known model for lattice bosons is the Bose-Hubbard model [16], which involves tight-binding physics in the presence of interactions and yields a superfluid-Mott insulator transition driven by the competition between localization and itineracy. In this paper, we report our findings of a phase diagram of imbalanced fermions in lattice tubes that displays a high resemblance to the Bose-Hubbard phase diagram. Figure 1b shows a contour plot of average tube-filling imbalance (number difference between the two species in a tube), M , as a function of the chemical potential difference (or the magnetic field), h , and the intertube tunneling, t . With the decrease in t across a critical value, the system undergoes a magnetic compressible-incompressible transition, with

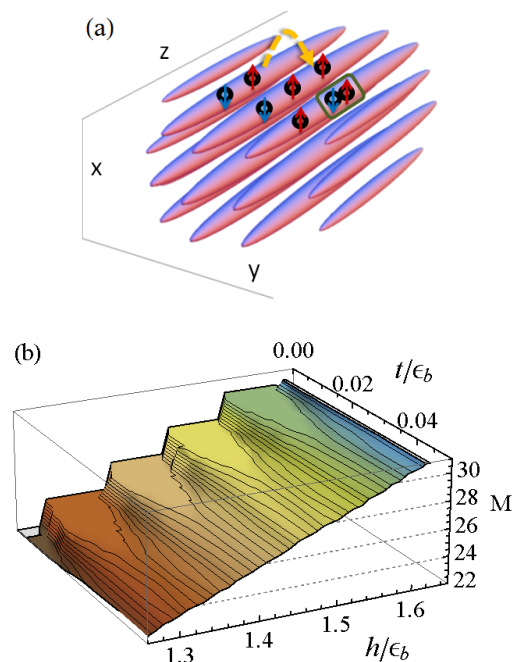


FIG. 1: (Color Online) (a) Illustration of a 2D array of tubes in a global 3D trapping potential, filled with \uparrow and \downarrow fermions. The dashed arrow indicates particle tunneling between tubes, while the enclosed pair represents the Cooper pairing. (b) Filling imbalance per tube, M , in a radially uniform system as a function of chemical potential difference (or magnetic field), h , and intertube tunneling, t (obtained from the corresponding BdG calculations). The lobe-like plateaus represent a magnetic incompressible state with corresponding integer fillings, while the outside regions have finite compressibility, $\partial M/\partial h$.

the compressibility, $\partial M/\partial h$, going from a finite value to zero, accompanied with M changing from fractional to integer occupations. In the Bose-Hubbard model it is the site-filling number that undergoes a transition between compressible (superfluid) and incompressible (Mott insulator) states. This similarity implies a bosonic behavior

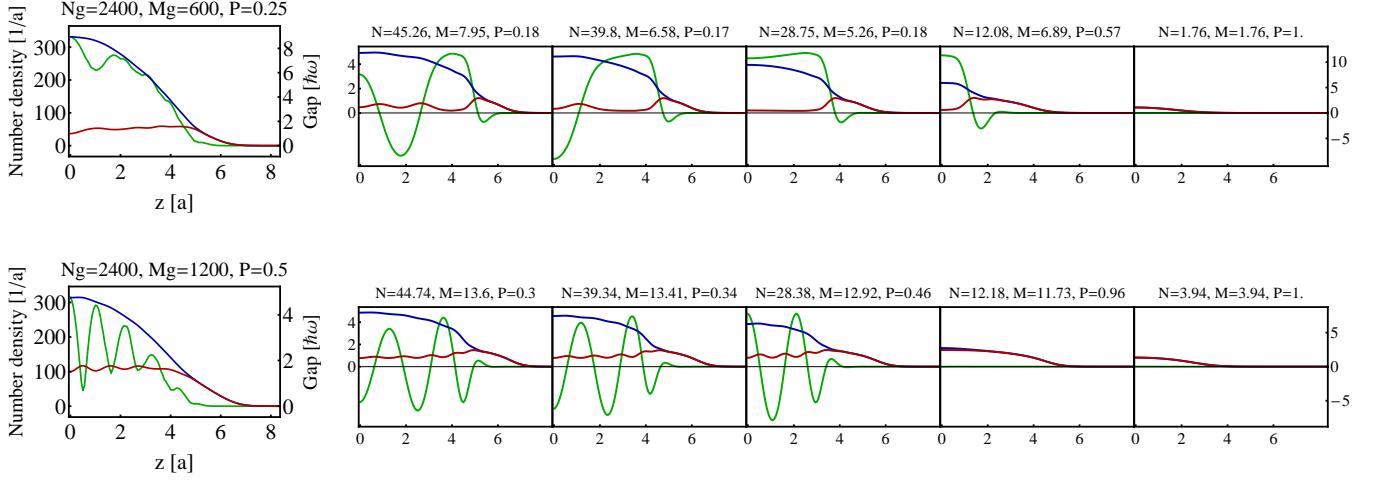


FIG. 2: (Color Online) Left: axial profiles of total density ρ , spin imbalance s (blue and red curves, respectively, axis on left-hand side of graph), and average magnitude of pairing gap $|\Delta|$ (green curve, axis on right-hand side of graph). Right: corresponding profiles of single tubes located in the diagonal from the center (left figure) to the edge (right figure) of the array (represented as the left, except the sign of pairing gap is revealed). The first and second rows represent systems of 25% and 50% global polarization, respectively. Top labels show the number, the imbalance and the polarization of the corresponding density profiles. All profiles presented are even functions of z . The data obtained were for systems of 2400 particles in a 10×10 tube array with global trapping frequency $\omega = 0.0625\epsilon_b$ (which defines the oscillator length, a), tunneling $t = 0.014\epsilon_b$, and temperature $T = 0.1\epsilon_b$.

of the lattice tube fermions, which we explain below with a picture of the interplay between the intratube oscillatory pairing and the intertube coupling.

We begin with a study of spatial profiles of the system that display the FFLO physics. Then we turn to discuss the compressible-incompressible transition and its analogy to a Bose-Hubbard system. Finally, as a signature for this transition and hence (indirectly) for the oscillatory pairing, we investigate the linear response of the system to lattice modulations in cold atom experiments.

The trapped tube lattices filled with spin up/down fermions, $\hat{\psi}_{\sigma=\uparrow/\downarrow, \mathbf{r}}(z)$, are described by a microscopic Hamiltonian

$$H = \int_z \sum_{\mathbf{r}} \left(\sum_{\sigma} \hat{\psi}_{\sigma\mathbf{r}}^{\dagger} H_{\sigma}^0 \hat{\psi}_{\sigma\mathbf{r}} + g \hat{\psi}_{\uparrow\mathbf{r}}^{\dagger} \hat{\psi}_{\downarrow\mathbf{r}}^{\dagger} \hat{\psi}_{\downarrow\mathbf{r}} \hat{\psi}_{\uparrow\mathbf{r}} \right) - t \int_z \sum_{\langle \mathbf{r}\mathbf{r}' \rangle, \sigma} \hat{\psi}_{\sigma\mathbf{r}}^{\dagger} \hat{\psi}_{\sigma\mathbf{r}'}, \quad (1)$$

with the \hat{z} direction along the tube axis and $\mathbf{r} = (x, y)$ denoting different tubes (as illustrated in Fig. 1a). The one-particle Hamiltonian, $H_{\sigma}^0 = -(\hbar^2/2m)\partial_z^2 + m(\omega_r^2 r^2 + \omega_z^2 z^2)/2 - \mu_{\sigma}$, includes the kinetic energy in the \hat{z} direction, the global trapping potential and the chemical potential for each spin. The on-tube coupling constant is given as $g = 2\hbar^2 a_s / [m\ell^2(1 - 1.033a_s/\ell)]$ in the highly elongated tube limit, with a_s the two-body s-wave scattering length and ℓ the oscillator length of the transverse confinement in a tube [17]. The intertube tunneling, given by $t = \frac{4}{\sqrt{\pi}} E_R (V_0/E_R)^{3/4} \exp[-2\sqrt{V_0/E_R}]$ with V_0 the

optical-lattice depth and E_R the recoil energy [18], allows particles to move between nearest neighbor tubes, $\langle \mathbf{r}\mathbf{r}' \rangle$.

To analyze the system in the attractive interaction regime ($g < 0$), we apply a Bogoliubov-de Gennes (BdG) scheme [19] (that has been successfully used in the past to describe a variety of tube-confinement problems [9, 20–24] and is considered more reliable in the presence of intertube tunneling), with self-consistent treatment of the Hartree potential, $U_{\sigma} = g\rho_{-\sigma}$ where ρ_{σ} is the number density, and the BCS pairing field, $\Delta = g\langle \psi_{\downarrow}\psi_{\uparrow} \rangle$. The BdG mean-field Hamiltonian is thus written as

$$H_M = \int_z \sum_{\mathbf{r}} \left[\sum_{\sigma} \hat{\psi}_{\sigma\mathbf{r}}^{\dagger} (H_{\sigma}^0 + U_{\sigma}) \hat{\psi}_{\sigma\mathbf{r}} + (\Delta \hat{\psi}_{\uparrow\mathbf{r}}^{\dagger} \hat{\psi}_{\downarrow\mathbf{r}}^{\dagger} + \text{h.c.}) \right] - t \int_z \sum_{\langle \mathbf{r}\mathbf{r}' \rangle, \sigma} \hat{\psi}_{\sigma\mathbf{r}}^{\dagger} \hat{\psi}_{\sigma\mathbf{r}'}. \quad (2)$$

We perform a Bogoliubov transformation, $\hat{\psi}_{\sigma\mathbf{r}}(z) = \sum_n [u_{n\sigma\mathbf{r}}(z)\hat{\gamma}_{n\sigma} - \sigma v_{n\sigma\mathbf{r}}^*(z)\hat{\gamma}_{n,-\sigma}^{\dagger}]$, to rotate H_M to the quasiparticle eigenbasis. We numerically solve the BdG equation for self-consistent solutions of the quasiparticle wave functions, u and v , as well as their energy spectrum and hence obtain the spatial profiles for total density, $\rho = \rho_{\uparrow} + \rho_{\downarrow}$, spin imbalance (or magnetization), $s = \rho_{\uparrow} - \rho_{\downarrow}$, and pairing gap, Δ . The following results were obtained for an interaction strength set by choosing the binding energy $\epsilon_b \equiv mg^2/4\hbar^2 = 16\hbar\omega$.

We first look at the spin imbalance distribution and the appearance of oscillatory pairing in an isotropic trap

($\omega_r = \omega$). In Fig. 2, we plot the axial profiles of ρ , s and the average of $|\Delta|$ (left side of the figure) of the system after tracing out the \mathbf{r} degree of freedom; as well as the corresponding profiles in single tubes aligned in diagonal from the center to the edge of the array (right side). The first and second rows correspond to a lower global polarization of 25% (LP) and a higher one of 50% (HP), respectively. Here the polarization P is the ratio of the global imbalance, M_g , to the global number, N_g . We find that the imbalanced regions of tubes always accommodate oscillatory pairing (FFLO), with the concurrence of imbalance local maxima and gap nodes, except for the gap decaying to zero in entering a fully polarized region ($\rho = s$). In the LP case, single-tube profiles in the \hat{z} direction can exhibit an FFLO-pairing center, a BCS-like fully paired off-center region ($s \sim 0$ and no gap nodes) and fully polarized tails. A similar trend is seen in the \hat{r} direction: center tubes with a larger FFLO region, off-center tubes with a larger BCS-like region, and fully polarized edge tubes. The oscillatory pairing behavior is also revealed by the sign changes at fixed z across the tubes. In the HP case, the structure of an FFLO center and fully polarized tails remains, except the BCS-like regions disappear.

The axial profiles of both the spin imbalance and the pairing gap in the HP case exhibit a clearer oscillation than those in the LP case. This indicates an alignment of the gap nodes (occupied by unpaired majority spins) across the tubes and hence implies a significant role of the intertube coupling (the particle tunneling in our model). To investigate the interplay between these parameters, we compute the total imbalance, M , (which also represents the occupation number of unpaired majority) per tube of a radially homogeneous system ($\omega_r = 0$) at zero temperature. Figure 1b shows a diagram of M as a function of intertube tunneling, t , and chemical potential difference, h . It exhibits a remarkable similarity to the phase diagram of the Bose-Hubbard model [16], which describes a lattice system of interacting bosons. A salient feature of the Bose-Hubbard model is the existence of a quantum phase transition between an incompressible Mott insulator with integer fillings and a compressible Bose-Einstein condensate with fractional site occupations, driven by an energetic competition between tunneling and interaction. Our tube system, in analogy, possesses a magnetic compressible-incompressible transition, with the two phases identified by the filling of imbalance and the compressibility, $\partial M/\partial h$. At small tunneling, an increase of the magnetic field, h , moves the system from an incompressible state (one of the lobe-like plateaux in Fig. 1b) to another one with different filling integer, across a narrow compressible region. If we begin with a fixed filling integer, with an increase in tunneling the corresponding plateau shrinks until a critical tunneling (the tip of the lobe), beyond which the system enters the compressible regime; with still an integer filling.

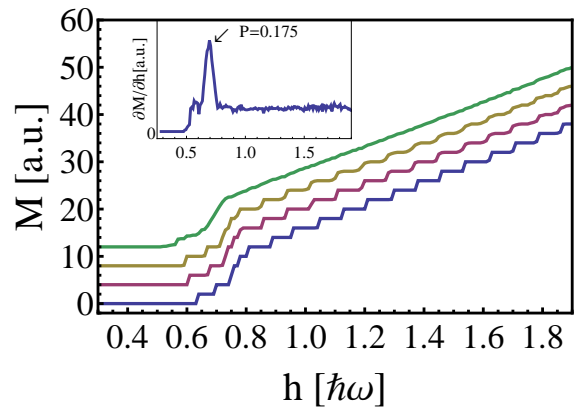


FIG. 3: (Color Online) Imbalance per tube, M , vs magnetic field, h at various tunneling strengths. Curves from bottom to top correspond to $t/\epsilon_b = 0.003, 0.014, 0.02$ and 0.05 (or the lattice depth $V_0/E_R = 12, 7, 6$ and 3.8 , respectively), with the top three curves shifted up. Inset: $\partial M/\partial h = 0$ vs h at $t = 0.05\epsilon_b$. A λ -like transition appears around $P = 17.5\%$. At small t the curves display the same trend but with staggered substructures. The data obtained were for systems of 2560 particles in an 8×8 array of tubes at zero temperature.

Figure 3 shows the M - h curves at several tunneling strengths (the corresponding section profiles of Fig. 1b) in a wide range of h . We see that in the low- h regime the whole system is a BCS superfluid ($M = 0$) and the FFLO sets in at a critical h beyond which M becomes finite. In the relatively low polarization regime ($P = 10\%$ – 20% , around $h = 0.7\hbar\omega$), the compressibility displays a λ -like transition with a peak corresponding to $P = 17.5\%$ (see inset), which agrees with the critical polarization for the disappearance of BCS-like outer regions in the experiment [15]. Our data show that this critical polarization is insensitive to the strength of intertube tunneling.

Let us discuss a difference between our system and the Bose-Hubbard model: the filling integer between two neighboring plateaux jumps by two in our system whereas it jumps by one in the Bose-Hubbard model. Since the trapping potential as an even function of z conserves the parity symmetry of the gap profile [23], there are even/odd nodal solutions capable of accommodating an even/odd number of unpaired majority spins per tube in an incompressible state. Although the results presented in this paper are for the even solutions, we find also the odd ones exhibiting the same Bose-Hubbard-like diagram. In either case, the integer filling jumps by two.

In addition, we find the system prefers all the tubes of the same parity, otherwise an energy cost will arise due to the formation of domain walls between tubes of opposite parities. Such energy cost not only prohibits the system to globally “flip” between opposite parities but also suppresses the single-particle tunneling of the unpaired majority spins. Therefore, the leading behavior remaining is a two-body tunneling that conserves the

tube parity. This bosonic nature allows us to write down an effective Bose-Hubbard Hamiltonian for the system,

$$H_{\text{eff}} = -\tilde{t} \sum_{\langle \mathbf{r}\mathbf{r}' \rangle} \hat{b}_{\mathbf{r}}^\dagger \hat{b}_{\mathbf{r}'} + \sum_{\mathbf{r}} \tilde{E}(\hat{M}_{\mathbf{r}}) - h\hat{M}_{\mathbf{r}}, \quad (3)$$

where \hat{b}^\dagger creates two unpaired majority spins while preserving parity and $\hat{M} = \hat{b}^\dagger \hat{b}$ is the imbalance operator of a fixed parity. The effective tunneling, \tilde{t} , is estimated as the ratio of t^2 to the domain wall energy, while the effective on-tube interaction \tilde{E} should be a non-linear function in \hat{M} . Assuming that $\tilde{E}(\hat{M}) \sim (\tilde{U}/2)\hat{M}^2$ takes a quadratic form, the mean-field solution of H_{eff} shows that in the weak tunneling limit the width of an incompressible lobe gives \tilde{U} and the narrow compressible layer between two lobes is $2(M+1)Z\tilde{t}$ [25], with the coordination number $Z = 4$ for the 2D array. Fitting the numerical data in Fig. 1b, We find the effective coupling $\tilde{U} \sim 0.08\epsilon_b$ and $\tilde{t} \sim 0.024t$. For a single uniform tube, analytic limits of the on-tube energy have been discussed in Ref. [26], taking a form of quadratic or higher order in \hat{M} . Because the interaction plays a key role in the phase transition in the Bose-Hubbard model, this magnetic compressible-incompressible transition is different from the commensurate-incommensurate transition identified in Ref. [9] that is interpreted as band filling of unpaired majority spins. These two different scenarios for the gapped states, analogous to the difference between the band insulator (cf. Ref. [9]) and the Mott insulator (here), could come from differences in the two setups considered. For example, a setup of homogeneous tubes and periodic boundaries in Ref. [9] may favor a pairing function in the plane wave basis (FF-type), while a trap confinement in our setup naturally conserves the parity symmetry of the pairing in real space (LO-type). In addition, the parameter regimes considered in these two studies are also different.

We now turn to the issue of probing such transition in experiments. A salient characteristic of an incompressible state is that the energy spectrum exhibits a gap between the ground state energy and the low excitations, which is not present in a compressible state. A realizable technique to explore the excitation spectrum is to detect the response of the lattice system to a time periodic modulation of the lattice depth. This probe has been successfully applied to distinguish an incompressible state from a compressible one in cold atom experiments of quasi-1D lattice bosons [27] and 3D lattice fermions [28].

For our lattice of tubes, we calculate the linear response of the imbalance in the “hidden” dimension of the 2D array – the axial profile, $\delta s(z)$ – to a modulation in tunneling strength, which can be induced by modulating the lattice depth. We obtain $\delta s(z, \omega_m)$ in the frequency domain as

$$\sum_{n < 0, n' > 0} A_{nn'} \delta(\epsilon_{n'} - \epsilon_n - \hbar\omega_m) \sum_{\mathbf{r}} (v_{n\downarrow}^* v_{n'\downarrow} + u_{n\uparrow}^* u_{n'\uparrow})$$

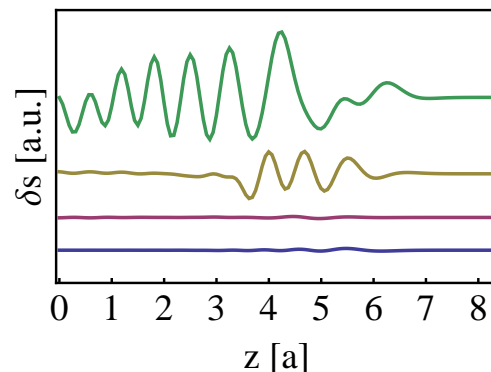


FIG. 4: (Color Online) Response of imbalance (magnetization) axial profile to tunneling modulation around $\omega_m = \omega$. Curves from bottom to top correspond to $t/\epsilon_b = 0.003, 0.014, 0.02$ and 0.05 , with each of the top three curves shifted up (as illustrated in Fig. 3). A large (small) response indicates a compressible (incompressible) states.

where ϵ_n are quasiparticle eigenenergies and ω_m is the modulation frequency. The amplitude $A_{nn'} \propto \int_z \sum_{\langle \mathbf{r}\mathbf{r}' \rangle} (v_{n'\downarrow}^* v_{n\downarrow} - u_{n'\uparrow}^* u_{n\uparrow})$, combined with the orthogonality between quasiparticle wave functions, guarantees that $\delta s(z)$ has even parity in z and conserves the total imbalance ($\int_z \delta s = 0$).

To reflect the natural inhomogeneity in experiments, we present our results for a trapped setup, as in Fig. 2, of 50% polarization and at a low temperature ($T = 0.01\epsilon_b$). Figure 4 shows δs at four different tunneling strengths, those illustrated for a radially homogeneous case in Fig. 3. It can be seen that in the incompressible regime where the M - h curves display a staggered structure, the imbalance profile has little response ($\delta s \sim 0$), while in the compressible regime δs shows larger features signaling a strong response. Notice that our results are robust against fluctuations in total numbers coming from the Josephson coupling between tubes, due to the nature of the BdG Hamiltonian that conserves the total spin imbalance.

In conclusion, we identified an interesting transition in a lattice array of tubes with a strong analogy to the extensively studied compressible-incompressible transition in the Bose-Hubbard model. In our fermionic system, the underlying reason for the effective bosonic behavior is crucially linked to the oscillatory nature of the pairing amplitude. The observation of this transition would thus constitute an additional evidence of the FFLO state hinted by recent experiments. Our prediction of easily accessible experimental signatures is quite encouraging and this transition deserves further theoretical and experimental investigation.

We are grateful to L. O. Baksmaty, R. Hulet, and S. Vishveshwara for interesting discussions. This work was supported by the DARPA-ARO Award No. W911NF-07-1-0464.

-
- [1] I. Bloch, J. Dalibard, and W. Zwerger, *Rev. Mod. Phys.* **80**, 885 (2008).
- [2] C. Chin, R. Grimm, P. Julienne, and E. Tiesinga, *Rev. Mod. Phys.* **82**, 1225 (2010).
- [3] W. Ketterle and M. Zwierlein, *Nuovo Cimento* **031**, 247 (2008).
- [4] S. Giorgini, L. P. Pitaevskii, and S. Stringari, *Rev. Mod. Phys.* **80**, 1215 (2008).
- [5] L. Radzihovsky and D. E. Sheehy, *Rep. Prog. Phys.* **73**, 076501 (2010).
- [6] P. Fulde and R. A. Ferrell, *Phys. Rev.* **135**, A550 (1964).
- [7] A. I. Larkin and Yu. N. Ovchinnikov, *Zh. Eksp. Teor. Fiz.* **47**, 1136 (1964) [*Sov. Phys. JETP* **20**, 762 (1965)].
- [8] K. Yang, *Phys. Rev. B* **63**, 140511(R) (2001).
- [9] M. M. Parish, S. K. Baur, E. J. Mueller, and D. A. Huse, *Phys. Rev. Lett.* **99**, 250403 (2007).
- [10] E. Zhao and W. V. Liu, *Physical Review A* **78**, 063605 (2008).
- [11] A. E. Feiguin and F. Heidrich-Meisner, *Phys. Rev. Lett.* **102**, 076403 (2009).
- [12] J. P. A. Devreese, S. N. Klimin and J. Tempere, *Phys. Rev. A* **83**, 013606 (2011).
- [13] R. M. Lutchyn, M. Dzero, and V. M. Yakovenko, *Phys. Rev. A* **84**, 033609 (2011).
- [14] H. Moritz, T. Stöferle, K. Günter, M. Köhl, and T. Esslinger, *Phys. Rev. Lett.* **94**, 210401 (2005).
- [15] Y. Liao, A. S. C. Rittner, T. Paprotta, W. Li, G. B. Partridge, R. G. Hulet, S. K. Baur, and E. J. Mueller, *Nature* **467**, 567 (2010).
- [16] M. P. A. Fisher, P. B. Weichman, G. Grinstein, and D. S. Fisher, *Phys. Rev. B* **40**, 546 (1989).
- [17] M. Olshanii, *Phys. Rev. Lett.* **81**, 938 (1998).
- [18] H. P. Büchler, G. Blatter, and W. Zwerger, *Phys. Rev. Lett.* **90**, 130401 (2003).
- [19] P. G. De Gennes, *Superconductivity of Metals and Alloys* (Addison-Wesley, Reading, MA, 1989).
- [20] T. Mizushima, K. Machida, and M. Ichioka, *Phys. Rev. Lett.* **94**, 060404 (2005).
- [21] X.-Ji Liu, H. Hu, and P. D. Drummond, *Phys. Rev. A* **76**, 043605 (2007); *Physical Review A* **78**, 023601 (2008).
- [22] L. O. Baksmaty, H. Lu, C. J. Bolech, and H. Pu, *Phys. Rev. A* **83**, 023604 (2011); *New J. Phys.* **13**, 055014 (2011).
- [23] K. Sun, J. S. Meyer, D. E. Sheehy, and S. Vishveshwara, *Phys. Rev. A* **83**, 033608 (2011).
- [24] L. Jiang, L. O. Baksmaty, H. Hu, Y. Chen, and H. Pu, *Phys. Rev. A* **83**, 061604(R) (2011).
- [25] K. Sun, C. Lannert, and S. Vishveshwara, *Phys. Rev. A* **79**, 043422 (2009).
- [26] G. Orso, *Phys. Rev. Lett.* **98**, 070402 (2007).
- [27] T. Stöferle, H. Moritz, C. Schori, M. Köhl, and T. Esslinger, *Phys. Rev. Lett.* **92**, 130403 (2004).
- [28] R. Jördens, N. Strohmaier, K. Günter, H. Moritz, and T. Esslinger, *Nature* **455**, 204 (2008).